WIND ENERGY
Wind Energ. 2014; **00**:1–22
DOI: 10.1002/we

RESEARCH ARTICLE

Adjustment of wind farm power output through flexible turbine operation using wind farm control

Sung-ho Hur[1] and William E. Leithead[1]

[1]Department of Electronic and Electrical Engineering, University of Strathclyde, Glasgow G1 1XW, UK

ABSTRACT

When the installed capacity of wind power becomes high, the power generated by wind farms can no longer simply be that dictated by the wind speed. With sufficiently high penetration, it will be necessary for wind farms to provide assistance with supply-demand matching. The work presented here introduces a wind farm controller that regulates the power generated by the wind farm to match the grid requirements by causing the power generated by each turbine to be adjusted. Further benefits include fast response to reach the wind farm power demanded, flexibility, little fluctuation in the wind farm power output and provision of synthetic inertia. Copyright © 2014 John Wiley & Sons, Ltd.

KEYWORDS

wind farm power control; wind turbine control; flexible turbine operation.

Correspondence

S. Hur, Department of Electronic and Electrical Engineering, University of Strathclyde, Glasgow G1 1XW, UK. E-mail: hur.s.h@ieee.org

Contract/grant sponsor

Supergen Wind Energy Technologies Consortium/Engineering and Physical Sciences Research Council

Contract/grant number

EP/H018662/1

Received . . .

1. INTRODUCTION

The 2013 statistic publication [1] by the European Wind Energy Association (EWEA) reports that there are 117.3 GW of installed wind energy capacity in the European Union (EU). With high penetration of wind power, the power generated by wind farms can no longer simply be that dictated by the wind speed. The operation of some *wind turbines* is already being curtailed [2, 3]. It will be necessary for *wind farms* to provide services to the grid including spinning reserve, frequency support and assistance with supply-demand matching. In these circumstances, to regulate the power generated by the wind farm to match the grid requirements, a wind farm controller, causing the power generated by each turbine to be adjusted, is required. A detailed survey on the recent development of wind farm control can be found in [4]. It is stated in the paper that wind farm control can be divided into two categories, those to maximise the aggregated wind farm power output [5] and those to follow a reference for the aggregated wind farm power output [6], both taking into account fatigue loading on

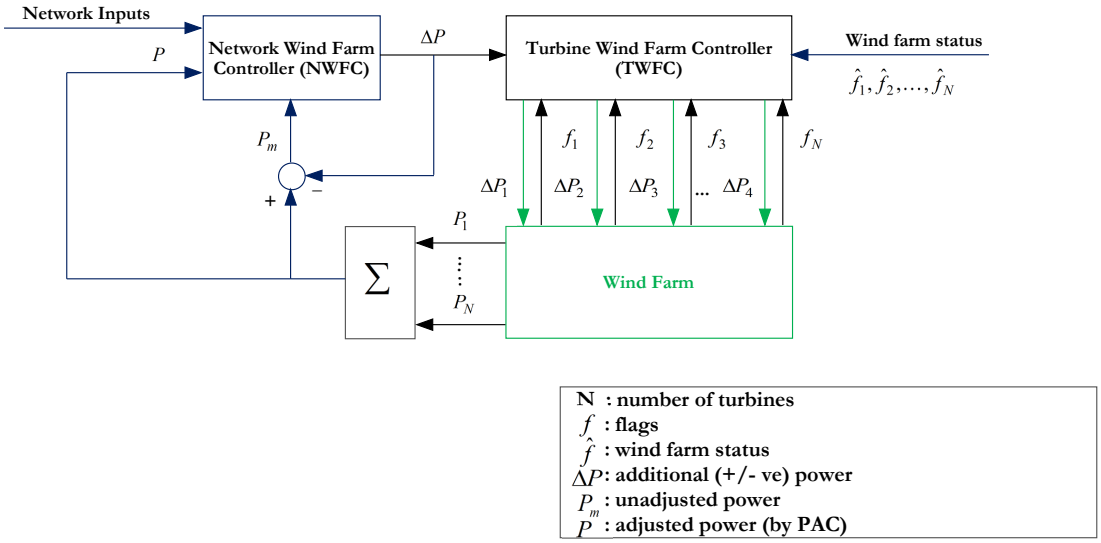

Figure 1. The structure of the wind farm controller.

the wind turbines. A flexible, hierarchic, decentralised and scalable approach to wind farm control that is pertinent to both the categories is introduced here. It is capable of providing fast and accurate control of the power generated by the wind farm in the below and above rated wind speed without compromising the turbines' own full envelope controllers through enclosing them in an additional feedback.

The structure of the wind farm controller is shown in Figure 1. It has two elements, the Network Wind Farm Controller (NWFC) and the Turbine Wind Farm Controller (TWFC). The NWFC acts on information regarding the state of the power network to determine the required power output from the wind farm and so the adjustment (ΔP) relative to P_m, the wind speed dictated output that would arise with no adjustment. The TWFC acts on information regarding the state of the wind farm and the turbines therein to allocate adjustments to each turbine, ΔP_i (for $i = 1, \ldots, N$, where N is the number of turbines in the farm) relative to the wind speed dictated output of turbine i.

Each wind turbine in the farm has its own full operational envelope controller [7] that ensures the wind turbine follows its required operating strategy and remains in a safe operating condition through regulating rotor speed, torque and some loads. Since the wind farm controller requires each turbine to adjust its power output on request, the full envelope controller is modified by addition of a Power Adjusting Controller (PAC) [8]. The summary of the PAC is included in Appendix A of this paper. As described in the appendix, the PAC causes the turbine to adjust its generated power by a demanded amount relative to that dictated by the wind speed. As the PAC is essentially a feed-forward controller, jacketing the full envelope controller, it does not compromise the operation of the full envelope controller. Hence, redesigning or retuning of the existing full envelope controller is not necessary. Furthermore, the PAC is sufficiently fast acting to provide the turbine with a synthetic inertia response [9, 10], but that usage of the PAC is not discussed in this paper.

To prevent the introduction of feedback loops between the wind farm controller and the individual turbines as depicted in Figure 1, the only communication regarding the state of each turbine to the wind farm controller is through "flags", f_i (for $i = 1, \ldots, N$). Furthermore, since the wind farm consists of a large number of turbines, the wind farm controller feedback acting on the total power output from the farm only introduces very weak feedback on each turbine. That is, as the number of turbines that share the adjustments to the wind farm power output increases, the feedback effect decreases, causing the wind farm controller to act independently from the controllers of the wind turbines.

The purpose of this paper is to investigate the design and performance of the wind farm controller in Figure 1 with the objective of operating the wind farm at some specified output power by allocating the individual adjustments to each turbine. The design of the wind farm controller is introduced in Section 2. Simulation results are presented in Section 3

Wind Energ. 2014; **00**:1–22 © 2014 John Wiley & Sons, Ltd.
DOI: 10.1002/we
Prepared using weauth.cls

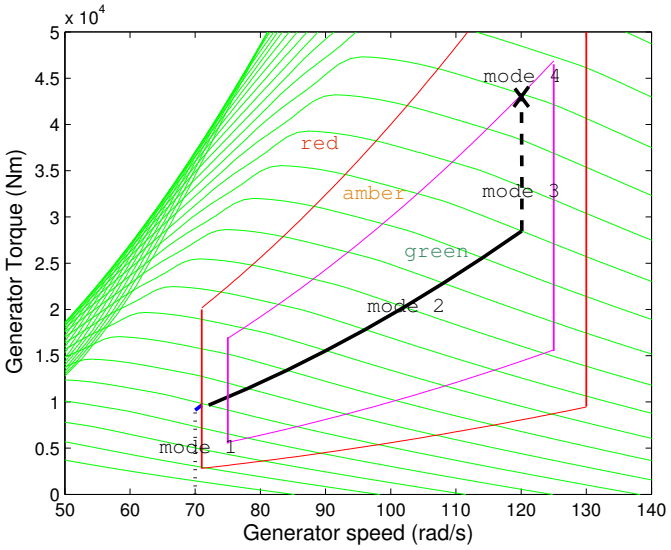

Figure 2. Design operating curve and operating regions (i.e. red, amber and green zones) defined by the thresholds over the full envelope operation on the torque/speed plane.

by applying the wind farm controller to a wind farm model. The wind farm is modelled using both Matlab/SIMULINK® and DNV GL Bladed (BLADED). The turbines are the Supergen (Sustainable Power Generation and Supply) Wind 5 MW exemplar wind turbine. The performance of the wind farm controller is analysed in more detail (e.g. in the frequency domain) in Section 4, and conclusions are drawn in Section 5.

2. WIND FARM CONTROL STRATEGY

The wind farm controller requires that each variable-speed pitch-regulated wind turbine be equipped with an existing full envelope controller and PAC. The full envelope controller causes the turbine to track its design operating curve as depicted on the torque/speed plane in Figure 2; that is, a constant generator speed (i.e. 70 rad/s) is maintained in the lowest wind speeds (mode 1); the C_{pmax} curve is tracked to maximise the aerodynamic efficiency in intermediate wind speeds (mode 2); another constant generator speed (i.e. 120 rad/s) is maintained in higher wind speeds (mode 3); and in above rated wind speed, the rated power of 5 MW is maintained by active pitching (mode 4) [11, 12].

The PAC provides fully flexible operation adjusting the power output from each turbine, more specifically, reducing the power for an unlimited time or increasing the power for a limited time if required, without altering the dynamics of the full envelope controller. However, if an increase or decrease in the power output is sustained, the turbine operating state could move away from the design operating curve.

The wind farm controller regulates the wind farm power output ensuring, at the same time, that each turbine (with the full envelope controller and PAC) operates within the safe operating region defined by the thresholds in Figure 2; that is, each turbine is prevented from going into unacceptable area, i.e. red zone as depicted in the figure, by the use of thresholds. In below rated wind speed, the turbines operating inside the inner thresholds, i.e. the green zone, could be allocated greater adjustments in power than the turbines operating outside the inner thresholds but inside the outer thresholds, i.e. the amber zone (in Figure 2, purple replaces amber for improved visibility in Matlab). The turbines operating outside the outer threshold, i.e. the red zone, will be allocated zero adjustment in power to bring them back onto the design operating curve.

In mathematical terms, these thresholds are determined on the generator torque (T_e)/generator speed (ω_g) plane [13] for convenience as

$$y_T = T_e - k_T \omega_g^2 \tag{1}$$

where k_T is a constant, unique for each threshold. For instance, with reference to the outer threshold (between the amber zone and the red zone) above the design strategy curve, y_T becoming positive indicates that the threshold has been crossed and the turbine is operating in the red zone, and vice versa. Hysteresis loops are incorporated into the thresholds to avoid chattering. Each hysteresis loop is asymmetric around the threshold, i.e. the distance from the threshold to the lower hysteresis limit is 10^3 (when switching from the red to amber zone) while the distance from the threshold to the upper hysteresis limit is 5 times larger (when switching from the amber to red zone) because it moves more rapidly from the amber to red zone than from the red to amber zone.

Based on these thresholds, flags are returned as 0, 1 or f_m. For the case investigated, setting f_m to 3 is suitable in modes 2, 3 and 4. In mode 1, the PAC is not activated. If a turbine is operating within the green zone (Figure 2), a flag of f_m would be returned. If a turbine is operating within the amber zone, a flag of 1 would be returned. Finally, if a turbine is operating within the red zone, a flag of 0 would be returned. ΔP_i with a flag of 0 would be zero, and ΔP_i with a flag of 3 would be 3 times larger than ΔP_i with a flag of 1.

The generation of the flags should be performed within the PAC rather than outside the PAC. Therefore, the PAC has been modified from the version reported in [8], and it now includes the flag generation feature as discussed in this section. The summary of the PAC included in Appendix A of this paper is up to date. Note that newer versions of the PAC should always include this feature. Other than this modification, the wind farm controller does not make any changes to the PAC; that is, the rest of the wind farm controller is developed outside the PAC.

The wind farm status could be determined by a number of factors including the health, age and location of the turbines. For instance, reduction in generated power may be made to only half the wind turbines in the farm, those on the up-wind side of the farm. The wind farm status, $\hat{f}_i$ (for $i = 0, 1, \ldots, N_T$) is also returned as 0, 1 or f_m. In turn, $\hat{f}_i$ and f_i are compared and the minimum is exploited in equation (4). However, it is assumed that every turbine has the same status in this paper; that is, $\hat{f}_i = f_m$ (for all i and where $f_m = 3$ for the case studied here).

The NWFC calculates ΔP (in Figure 1) using the following proportional-integral (PI) controller:

$$\Delta P(t) = k_p(P_d(t) - P(t)) + k_i \int (P_d(t) - P(t))dt \tag{2}$$

subject to the actuator constraints, where $P(t)$ and $P_d(t)$ denote adjusted power and demanded power, respectively, and k_p and k_i are the tuning parameters. The structure of the PI controller with anti-windup is depicted in Figure 3. In order to prevent integral windup, ΔP is limited to be less than 40 % of the rated power. Note that the PAC should not be utilised to curtail the power output by more than 30 % in real life [8]. k_a in the figure is the tuning parameter for the anti-windup loop.

Consequently, unadjusted power, P_m (the wind speed dictated wind farm power output that would arise with no adjustment) would be

$$P_m = P - \Delta P \tag{3}$$

The TWFC distributes ΔP to each turbine as ΔP_i based on flags, f_i (status of each turbine) and $\hat{f}_i$ (wind farm status as depicted in Figure 1) as follows

$$\Delta P_i = \frac{\Delta P \min(f_i, \hat{f}_i)}{\sum_{j=1}^{N_T} \min(f_j, \hat{f}_j)} \tag{4}$$

Wind Energ. 2014; **00**:1–22 © 2014 John Wiley & Sons, Ltd.
DOI: 10.1002/we
Prepared using weauth.cls

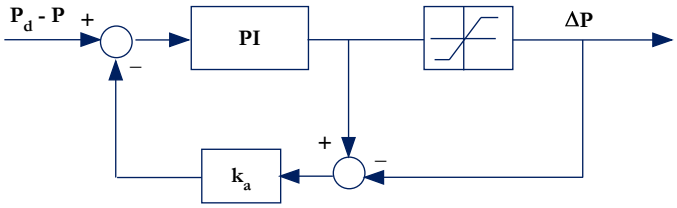

Figure 3. PI controller with anti-windup.

for $i = 1, \ldots, N$. The implication is that

$$\sum_{i=1}^{N_T} \Delta P_i = \Delta P \tag{5}$$

where N_T denotes the number of turbines in the wind farm. Equation (5) ensures that the power output from the wind farm tracks the demanded power even when the flags, hence ΔP_i, are being adjusted.

The allocation and reallocation of the power adjustment should take place in a smooth manner, which avoids the introduction of large transients, discontinuities and steps in the wind farm power output. It is achieved by filtering f_i (for $i = 0, 1, \ldots, N_T$) to ensure that the smoothing occurs only when crossing thresholds; that is, filtering f_i is equivalent to filtering ΔP_i only when crossing thresholds. A low pass filter, with time constant of 3 s, is exploited although the time constant could be larger in real life.

The full envelope controller ensures that the switching between the various modes (Figure 2) also takes place in a smooth manner.

3. SIMULATION RESULTS

Matlab/SIMULINK® and BLADED models of the Supergen 5 MW exemplar turbine, whose rated wind speed is approximately 11.5 m/s, are utilised. The Matlab/SIMULINK® model includes modules of aerodynamics, blades dynamics, rotor dynamics, actuator dynamics, drive-train, tower dynamics, generator, etc. and is reported alongside the full envelope controller in [7, 14] – each turbine model includes the full details reported therein, rather than being simplified. The parameters of the Supergen 5 MW exemplar turbine are used. The BLADED model provides greater details for the structural loads, while the Matlab/SIMULINK® model enables many turbines to be included in a wind farm model. The wind farm model thus consists of 9 Matlab/SIMULINK® models and 1 BLADED model. The two software packages are connected using StrathControl Gateway, a commercial software package that fully integrates the simulation. Due to the high computational demand, it is assumed that the wind farm contains only 10 turbines.

In this paper, as previously mentioned, it is assumed that every turbine has the same status except that they operate in different wind speeds. The different wind speeds cause the turbines to operate on different parts of the design operating curve (Figure 2).

A number of simulations have been conducted to demonstrate how the wind farm control strategy performs, and three of these simulations are reported in this section. In Simulation 1, ΔP is always negative in below rated wind speed. In Simulation 2, ΔP alternates between negative and positive values in below rated wind speed. In Simulation 3, ΔP is

always negative in just below rated wind speed that requires the full envelope controllers to switch between modes 2 and 3.

3.1. Wind Speed Model

The wind stochastically varies with time and continuously interacts with the rotor [15]. The effective wind speed is wind speed averaged over the rotor area such that the power spectrum of aerodynamic torque remains unchanged. In this paper, it is derived by filtering the point wind speed [16] through the filter introduced in [15]. The point wind speeds that take account of the correlation of the cluster layout and the wake effects are obtained from Bladed, thereby ensuring that the wind speeds are appropriately correlated. The effective wind speeds are required as inputs for the Matlab/SIMULINK® models. Bladed models include comprehensive models of complex wind fields to excite the turbine model, and the effective wind speed model is thus not required. By employing Bladed's built-in option, it is ensured that the wind speed that excites the turbine model is correlated with the effective wind speeds experienced by the Matlab/SIMULINK® models.

10 turbines are assumed to be aligned normally to the wind direction and evenly spaced 1 km apart, and the Bladed model represents the 5^{th} turbine in the cluster. In Figure 4, the correlated effective wind speeds at a mean wind speed of 8 m/s incorporated into the 9 Matlab/SIMULINK® models (the Bladed model representing the 5^{th} turbine) are depicted. Similar results can be expected at different mean wind speeds. Turbulence intensity of 10% is employed throughout this paper.

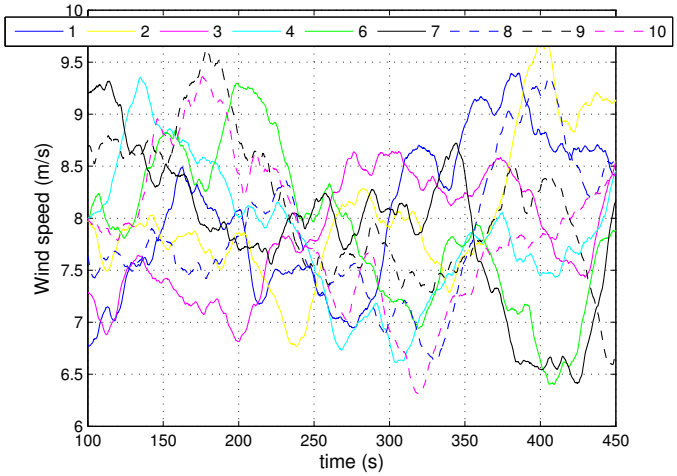

Figure 4. Wind speeds for turbines 1, 2, 3, 4, 6, 7, 8, 9, 10 at a mean wind speed of 8 m/s.

3.2. Simulation 1

In Simulation 1, the wind farm is required to produce a constant power of 12 MW at a mean wind speed of 8 m/s. Adjusted power in blue is depicted against unadjusted power in red in Figure 5. The PAC is switched on at 120 s past the transient response, and ΔP always remains negative.

Since it is the wind farm power output that is regulated, the individual power outputs from each turbine are still changing and being adjusted as depicted in Figure 6. The turbines experiencing lower wind speeds, for much of the time, generate less than 1.2 MW (demanded power output divided by the number of turbines, N), whilst those experiencing higher wind speeds, for much of the time, generate more than 1.2 MW. In total, a constant wind farm power output of 12 MW is produced as depicted in blue in Figure 5.

In the same situation, if the turbines were curtailed individually to 1.2 MW (subsequently adding the individual power outputs together to yield the wind farm power output), the individual power outputs would be reduced below 1.2 MW

DOI: 10.1002/we
Prepared using weauth.cls

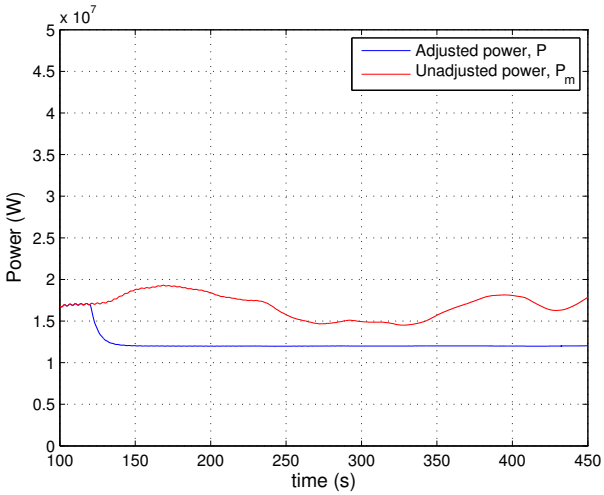

Figure 5. Simulation 1: adjusted vs unadjusted power.

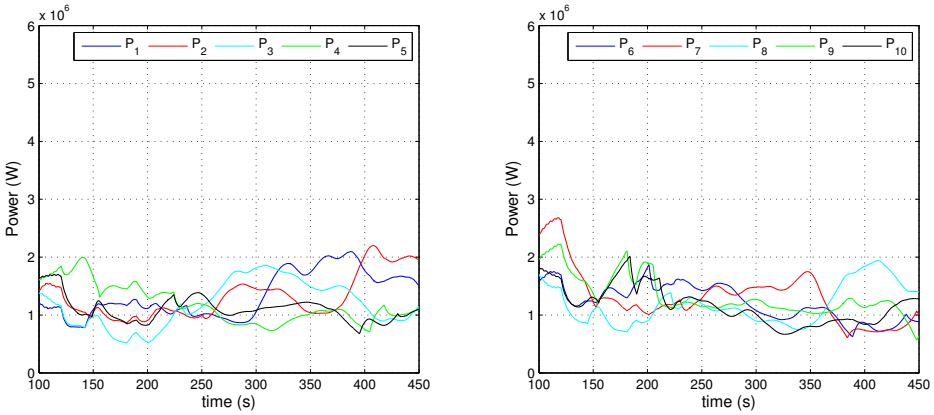

Figure 6. Simulation 1: power outputs from each turbine.

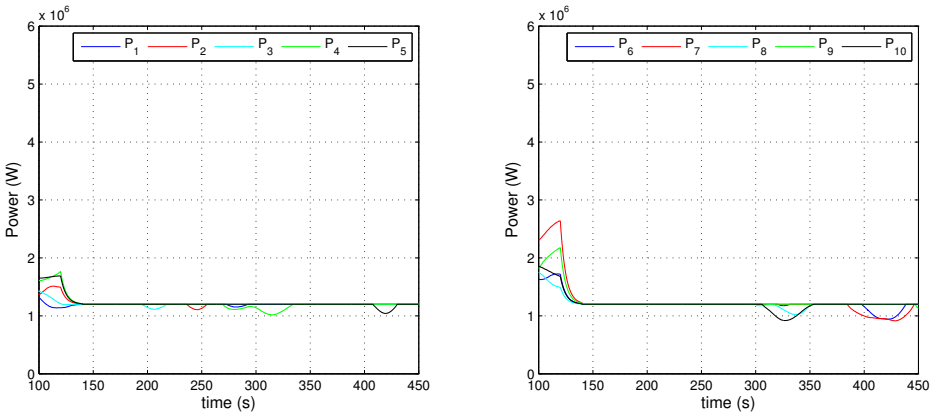

Figure 7. Individual curtailment: curtailed power outputs from each turbine.

when some turbines experience lower wind speeds as depicted in Figure 7. Consequently, as depicted in Figure 8, the

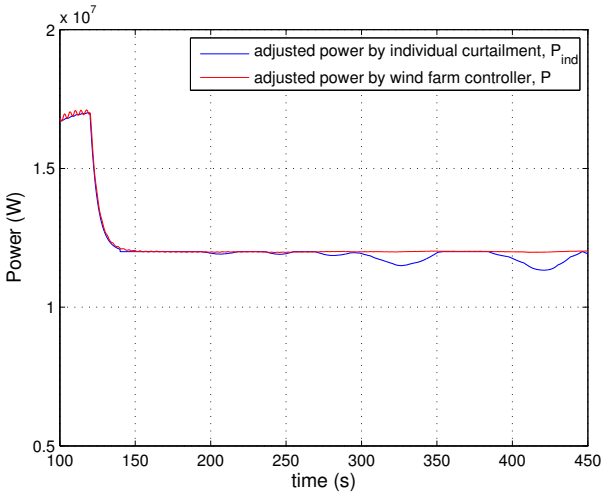

Figure 8. Adjusted power by individual curtailment vs adjusted power by the wind farm control strategy.

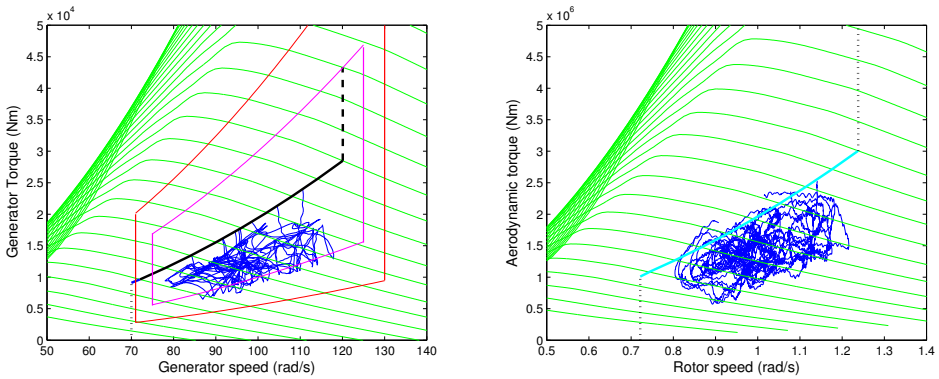

Figure 9. Simulation 1: behaviour of each turbine on the torque/speed planes.

output from the wind farm would, for much of the time, be less than 12 MW as depicted in blue against the adjusted power by the wind farm controller in red.

The performance of each turbine can be observed from Figure 9, which depicts T_f (left sub-figure) and T_e (right sub-figure) on the torque/speed planes from 100 to 450 s. The results demonstrate that the turbines operate within the green zone, allowing for the hysteresis loop. In more detail, when a turbine switches from the green zone to the amber zone, the turbine is allocated smaller adjustment in power, as the flag changes from 3 to 1, thereby causing the turbine to either slow down in moving towards the red zone or to return to the green zone. In this example, the turbines return to the green zone, and the red zone is never reached.

Despite all the allocation and reallocation of ΔP to each turbine as illustrated in Figures 6 and 9, a constant power of 12 MW is still maintained with little fluctuation as depicted in Figure 5.

3.3. Simulation 2

In Simulation 2, the wind farm is required to produce a constant power of 17 MW at a mean wind speed of 8 m/s. Adjusted power in blue is depicted against unadjusted power in red in Figure 10. The PAC is switched on at 120 s past the transient response. It depicts that ΔP alternates between positive (e.g., from approximately 420 to 440s) and negative (e.g., from approximately 125s to 235s) values. Although P can be held smaller than P_m ($\Delta P < 0$) for an unlimited time, P can

Wind Energ. 2014; **00**:1–22 © 2014 John Wiley & Sons, Ltd.
DOI: 10.1002/we
Prepared using weauth.cls

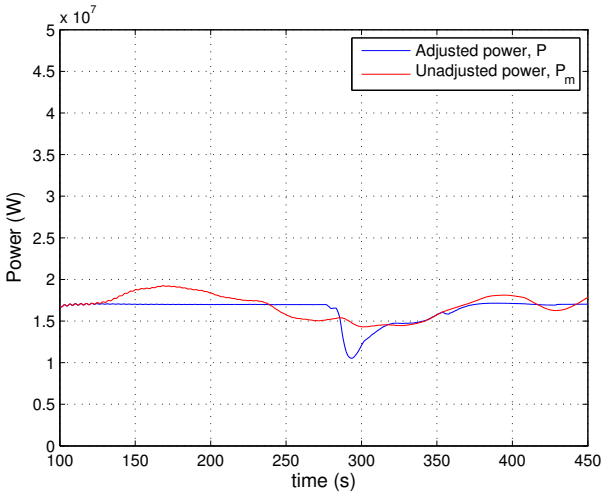

Figure 10. Simulation 2 when equations (4) and (5) are exploited; adjusted vs unadjusted power.

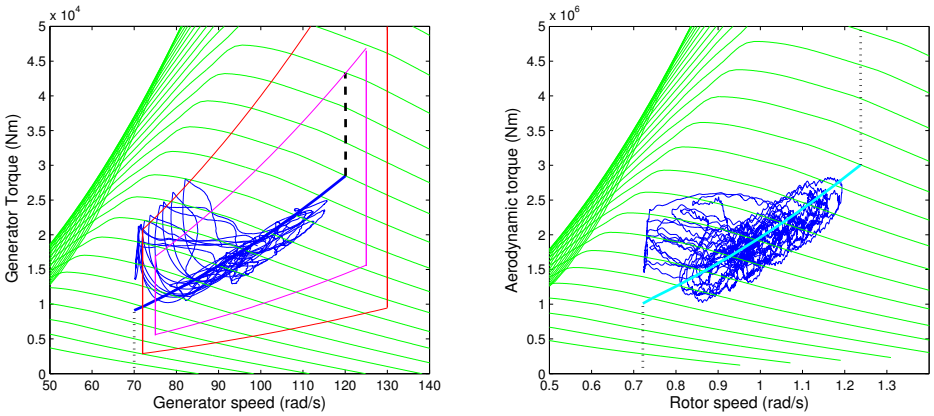

Figure 11. Simulation 2 when equations (4) and (5) are exploited; behaviour of each turbine on the torque/speed planes.

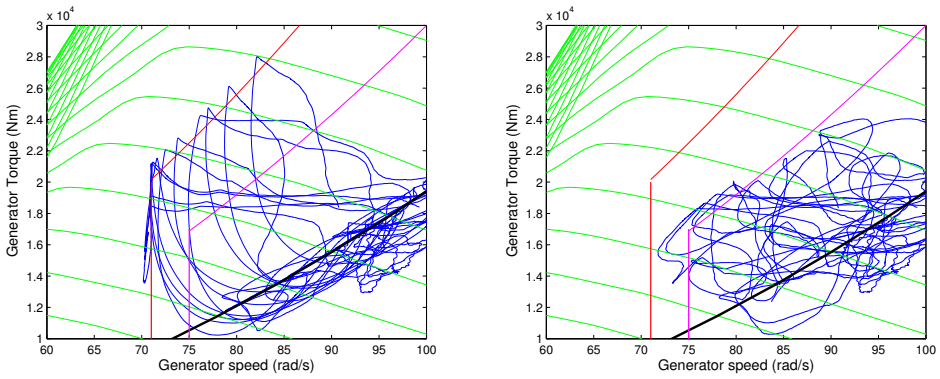

Figure 12. Left: zoomed version of Figure 11 (left) (before modification); right: zoomed version of Figure 13 (left) (after modification).

be held larger than P_m ($\Delta P > 0$) only for a limited time. Moreover, once the ΔP signal has been made positive, P is reduced by an appropriate amount from the wind speed dictated power output, P, until it is fully compensated (or recovered). More specifically, on occasions a requested $\Delta P > 0$ cannot be delivered by the turbine. In this situation, the

PAC rejects the request and places the turbine in the recovery mode setting the recovery flag to inform the wind farm controller [8]. Consequently, equation (5) can only be satisfied for a limited period of time when producing an additional power output.

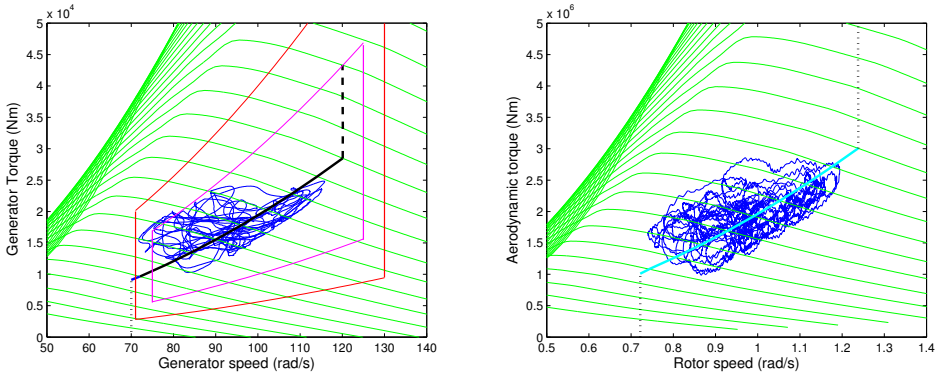

Figure 13. Behaviour of each turbine on the torque/speed planes.

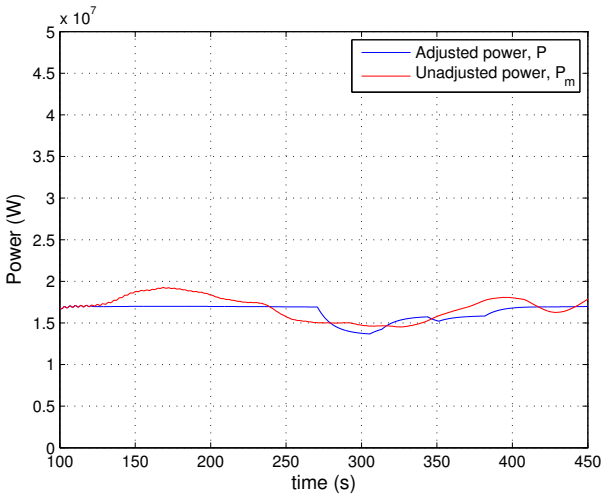

Figure 14. Simulation 2: adjusted vs unadjusted power after the modification.

The performance of each turbine can be observed from Figure 11, which depicts T_f (left sub-figure) and T_e (right sub-figure) on the torque/speed planes from 100 to 450 s. When turbine 1, for instance, enters the red zone, ΔP_1 would become zero to bring turbine 1 back to the green zone via the amber zone, and it would be in the recovery process [9]. Equation (4) causes ΔP_i of the remaining turbines to increase in order to compensate for turbine 1, i.e. trying to satisfy equation (5). As mentioned previously, the turbine operating state becomes much more sensitive when ΔP is positive, and as a result, the remaining turbines would speed up moving towards the red zone (due to the increase in ΔP_i). This process would repeat until every turbine cascades towards the red zone as depicted in Figure 11. A zoomed version of the left sub-figure of Figure 11 is depicted in Figure 12 (left sub-figure).

As every turbine is now going through the recovery process at the same time, a large dip in P is produced as depicted in Figure 10 (just after 270 s). As such a large dip would not satisfy the grid operation, a modification is made to equations (4) and (5) to prevent the remaining turbines from compensating for the turbine that has entered the amber/red zone when

DOI: 10.1002/we
Prepared using weauth.cls

producing an additional power output. Equation (2) is replaced with

$$\Delta P(t) = k_p(Q(t)P_d(t) - P(t)) + k_i \int (Q(t)P_d(t) - P(t))dt \tag{6}$$

where

$$Q(t) = \frac{\sum_{j=1}^{N_T} f_i(t)}{N_T f_m(t)} \tag{7}$$

With this modification, if every turbine is operating within the green zone, $Q(t)$ would be 1. If only one turbine enters the red zone (causing the turbine's flag to be 0), while the remaining turbines are still operating within the green zone (each of the remaining turbines having a flag of 3), Q would become $(30-3)/30$, reducing ΔP by $1/10$ in effect. This causes $P(t)$ to track the modified power demand, $Q(t)P_d(t)$, instead of $P_d(t)$.

Equation (5) now becomes

$$\sum_{i=1}^{N_T} \Delta P_i = Q\Delta P \tag{8}$$

only if ΔP is positive.

As a result of the modifications, when one turbine enters the amber zone in the same example, the remaining turbines do not attempt to compensate as depicted in Figure 13 (i.e. ΔP_i of the remaining turbines would not increase), no longer causing each turbine to cascade towards the red zone in succession. A zoomed version of the left sub-figure of Figure 13 is depicted in Figure 12 (right sub-figure) in comparison to the result from the same example before the modification is made (left sub-figure). The right sub-figure demonstrates that no turbine enters the red zone, and each turbine returns to the green zone as soon as it enters the amber zone. Consequently, the time response is also improved as depicted in Figure 14, i.e., the large dip shown in Figure 10 is no longer present.

When ΔP is negative such as in Sections 3.2 and 3.4, the turbine operating state is not as sensitive to the change in ΔP_i. Moreover, negative ΔP does not necessitate any recovery process [8] afterwards, and therefore, equation (4) can be safely exploited, hence satisfying equation (5).

3.4. Simulation 3

In Simulation 3, the wind farm is required to produce a constant power of 25 MW at a mean wind speed of 10 m/s. At this mean wind speed, the controller causes the turbines to switch between the C_{pmax} tracking (mode 2) and the constant speed (mode 3) operations. Adjusted power in blue is depicted against unadjusted power in red in Figure 15. The PAC is switched on at 120 s past the transient response. The performance of each turbine can be observed from Figures 16 and 17, which respectively depict T_f and T_e on the torque/speed planes.

The left sub-figure of Figure 16 demonstrates the operation of each turbine from 100 to 450 s, and the right sub-figure (zoomed) the operation of turbines 1, 2, 6 and 7 only from 350 to 400 s. To analyse the simulation results in more detail, attention is drawn to Turbines 1, 2, 6 and 7 in the right sub-figure. Turbines 1 and 2 operate in mode 3 while Turbines 6 and 7 operate in mode 2 just before 400 s. The figure depicts that Turbines 1 and 2 operate within the green zone while Turbines 6 and 7 enter the amber zone. Consequently, Turbines 6 and 7 should be reallocated a reduced power adjustment in comparison to Turbines 1 and 2. Figure 18 (just before 400 s) confirms that the reallocation takes place as expected at the switching region. As a result, turbines 6 and 7 re-enter the green zone as depicted in the figure.

Despite the allocation of reallocation of ΔP to each turbine, adjusted power is still smooth, avoiding the introduction of large transients, discontinuities and steps in the wind farm power output, as depicted (in blue) in Figure 15.

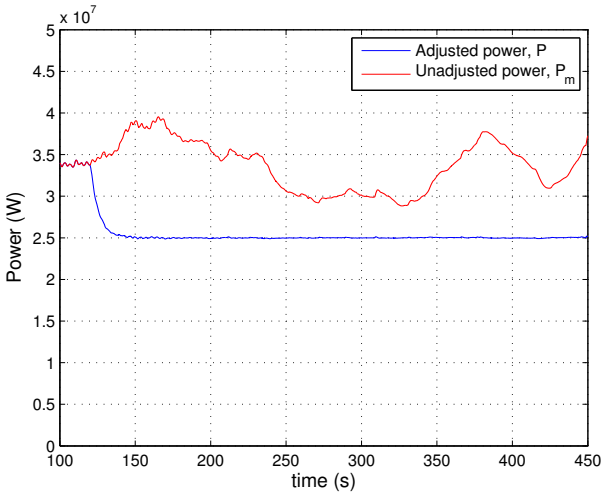

Figure 15. Simulation 3: adjusted vs unadjusted power.

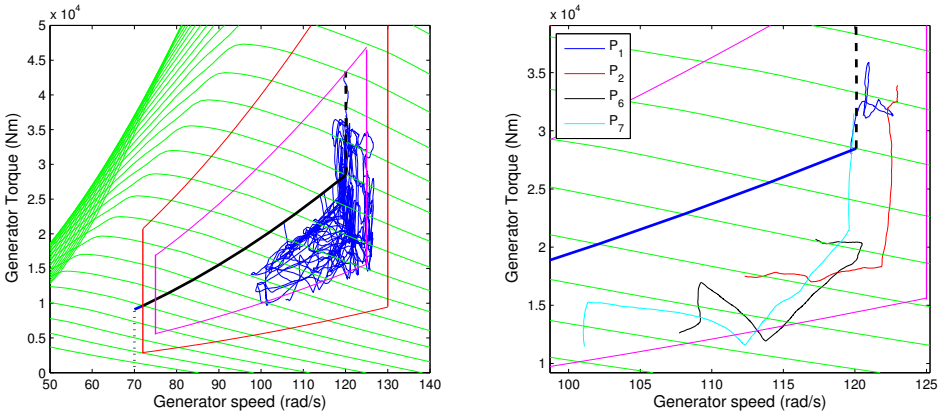

Figure 16. Simulation 3: behaviour of each turbine on the (generator) torque/speed plane; left sub-figure: turbines 1 to 10 from 100 to 450 s; right sub-figure: turbines 1, 2, 3 and 4 only from 350 to 400 s for the same example (zoomed).

4. PERFORMANCE ASSESSMENT

The performance assessment of the wind farm controller is carried out in more detail here by exploiting the results from simulation 3 in Section 3.4. In Section 4.1, mathematical proof and frequency analysis are presented to show that the operation of the wind farm controller and that of the individual turbines' full envelope controllers are independent. In Section 4.2, how increase in the number of turbines in the wind farm affects the difference between the wind farm power output and the power demand, which causes fluctuations, is examined. The speed of the wind farm controller is discussed in Section 4.3, and the effect of the communication delay that exists between the TWFC and the wind farm, as depicted in Figure 1, on the operation of the wind farm controller is investigated in Section 4.4.

Wind Energ. 2014; **00**:1–22 © 2014 John Wiley & Sons, Ltd.
DOI: 10.1002/we
Prepared using weauth.cls

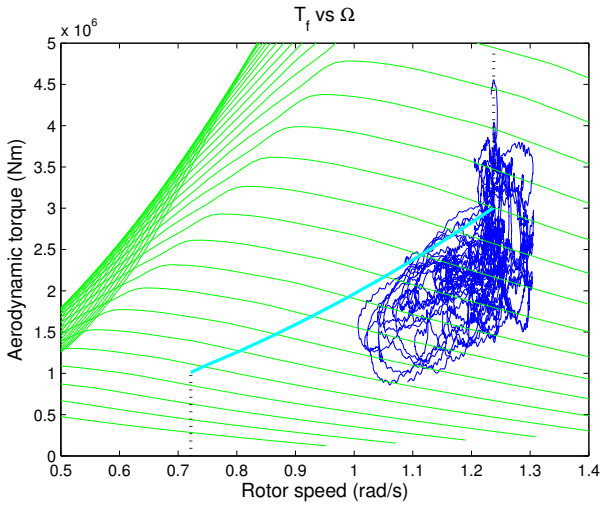

Figure 17. Simulation 3: behaviour of each turbine on the (hub) torque/speed plane.

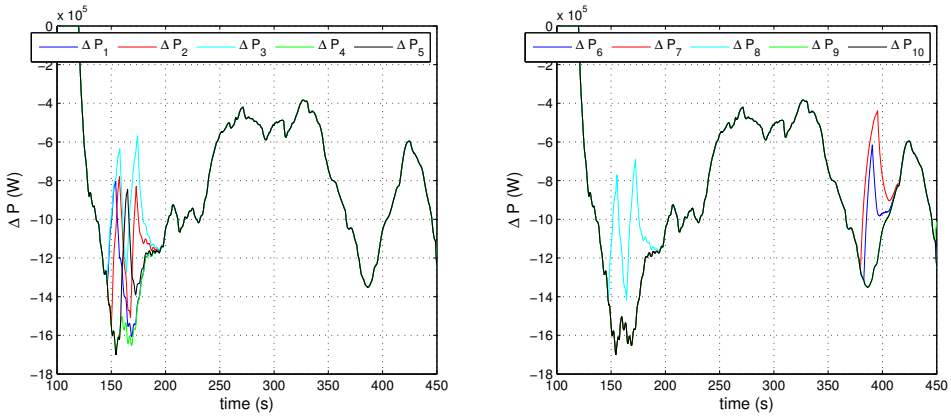

Figure 18. Simulation 3: adjustment in power; left sub-figure: turbines 1 to 5; right sub-figure: turbines 6 to 10.

4.1. Decoupling of the wind farm controller from the wind turbines controllers

It is important to ensure that the wind farm controller does not create a significant feedback effect on the individual wind turbine controllers. If a significant feedback effect is present, the effectiveness of the full envelope controllers could be impaired. It would then require retuning of the wind turbine controllers, rendering the wind farm controller less practical. It is shown in this sub-section that the feedback does not affect the operations of the individual wind turbine controllers.

The decoupling of the wind farm controller from the wind turbine controllers could be confirmed mathematically as follows. The full envelope controller of turbine 1, for instance, is designed to produce power output, P_1, to match the demanded power, $\tilde{P}_1$ such that

$$P_1 = \tilde{P}_1 \tag{9}$$

That is to say the equation is satisfied when the full envelope controller acts independently from the wind farm controller. However, with the introduction of the wind farm controller, a feedback effect is also introduced, modifying the equation as

$$P_1 = \tilde{P}_1 + \Delta P_1 \tag{10}$$

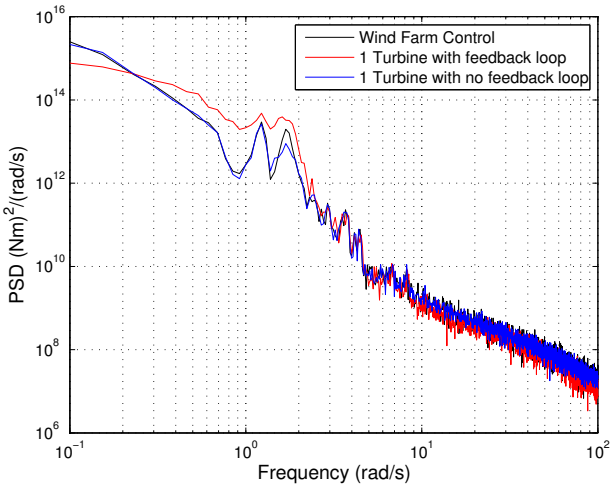

Figure 19. Simulation 3: spectrum of fore-aft (My) tower bending moment (black) in comparison to the situations with (red) and without (blue) a feedback effect.

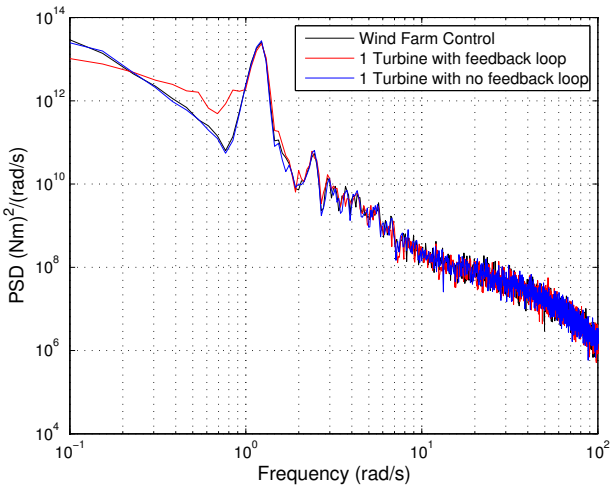

Figure 20. Simulation 3: spectrum of fore-aft (My) blade bending moment (black) in comparison to the situations with (red) and without (blue) a feedback effect.

assuming that ΔP from the NWFC is evenly allocated to each turbine, ΔP_1 in equation (10) is replaced with $\Delta P/N$.

It is clear that if the wind farm controller acts on 1 turbine only, equation (9) is no longer satisfied, and the wind farm controller is not decoupled from the wind turbine controller. However, for a large number of turbines in the wind farm, $\Delta P/N$ becomes negligible and equation (9) is satisfied, i.e. the wind farm controller is decoupled from the wind turbine controller. Thus, the wind farm controller does not alter the effectiveness of the full envelope controllers for a wind farm with a large number of turbines. Hence, the wind farm controller would be suitable for wind farms with a large number of turbines.

As previously mentioned, the decoupling of the wind farm controller from the wind turbine controller is further enhanced as the only communication regarding the state of each turbine to the wind farm controller is through "flags", f_i (for $i = 1, \ldots, N$). However, as there are only 10 turbines in the wind farm in this paper, the following experiments are performed to confirm that the actions of the wind farm controller and the wind turbine controllers are essentially independent even for a wind farm with 10 turbines by exploiting power spectra in the frequency domain as follows.

DOI: 10.1002/we
Prepared using weauth.cls

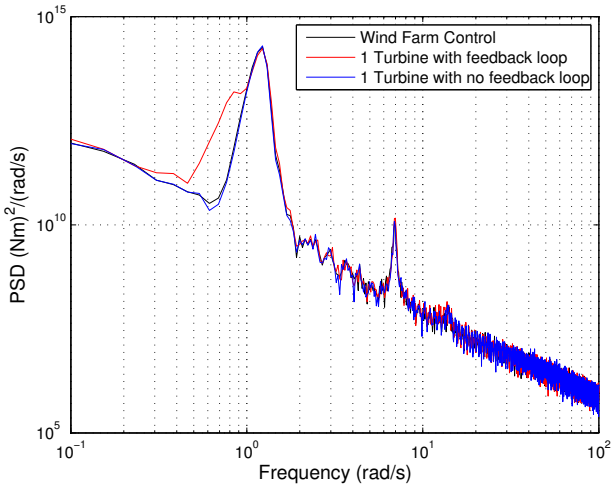

Figure 21. Simulation 3: spectrum of side-side (Mx) blade bending moment (black) in comparison to the situations with (red) and without (blue) a feedback effect.

It is much more convenient to confirm that the decoupling is indeed present in the frequency domain than in the time domain. In the time domain, the amplitude of any signal is dominated by the low frequency components making it problematic to discern any difference in behaviour at higher frequencies, where modifications to the full envelope controller behaviour would be evident. Hence the difference that would arise as a result is shown much more clearly in the frequency domain than in the time domain. Moreover, a significantly larger set of data would be required in the time domain than in the frequency domain.

For Simulation 3, the power spectra of fore-aft TBM, fore-aft BBM and side-to-side BBM are depicted in Figures 19, 20 and 21, respectively. The spectra for the situations with (red) and without (blue) a feedback effect are also depicted for comparison purposes. To simulate the situation with a feedback effect, the wind farm controller is applied to a single turbine model, and to simulate the situation without a feedback effect, a constant ΔP is applied with no feedback loop.

The results demonstrate that the power spectra for the situation with the wind farm controller (applied to the 10 turbine wind farm) and the power spectra for the situation with no feedback loop are analogous. It is, therefore, evident that the wind farm produces a constant power of 25 MW at a mean wind speed of 10 m/s, avoiding creating any significant feedback effect even for a wind farm with only 10 turbines. It implies that the actions of the wind farm controller and the wind turbine controllers are essentially independent. Almost identical results have been obtained for Simulations 1 and 2.

4.2. Increase in the number of turbines in the wind farm

Due to turbulence, the steady state power output adjusted by the wind farm controller would always fluctuate. Fluctuations, $V_r(t)$, due to the difference between $P(t)$ and $P_d(t)$ (in %) is defined as

$$V_r(t) = 100\frac{P(t) - P_d(t)}{P_d(t)} \tag{11}$$

where $P(t)$ and $P_d(t)$ denote adjusted power and demanded power, respectively.

$V_r(t)$ for the 10 turbine wind farm is depicted against $V_r(t)$ for a 5 turbine wind farm in Figure 22; 5 turbine wind farm is only exploited to provide a comparison, and its demanded power output is reduced by half. The comparison demonstrates that $V_r(t)$ is significantly smaller for the 10 turbine wind farm. The reduction in $V_r(t)$ from the 5 turbine to 10 turbine wind farm is also manifest in the power spectra depicted in Figure 23. In the figure, the overall amplitude is reduced for the

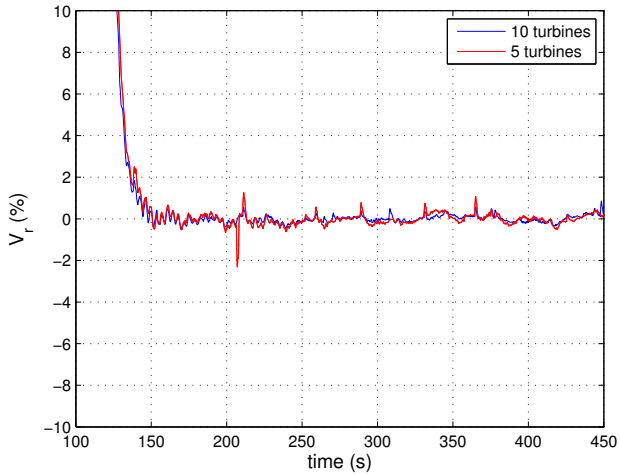

Figure 22. Fluctuations for 5 and 10 turbine wind farms for communication delay of 0.

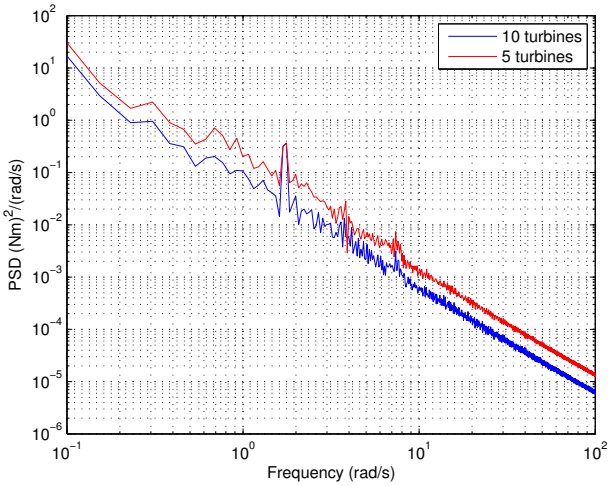

Figure 23. Spectra of fluctuations for 5 and 10 turbine wind farms for communication delay of 0.

10 turbine wind farm, while both the spectra exhibit similar characteristics. Hence, it could be inferred that $V_r(t)$ would be almost negligible for a wind farm with many tens of turbines.

4.3. Speed of the wind farm controller

Power adjustment by the wind farm controller is caused by adjustments in generator torque and pitch angle. Figure 24 illustrates that the adjustment in pitch angle takes place more slowly than the adjustment in torque (see [8]). Subsequently, the wind farm controller filters the resulting power adjustment through a low pass filter for smooth transitions. Figure 25 demonstrates that the speed of the wind farm controller could be adjusted by altering the time constant. Although time constant of 3 s has been used throughout the paper for smooth transitions, it could be increased or decreased when required. For instance, the wind farm controller would need to speed up when providing the turbines with a synthetic inertia response.

DOI: 10.1002/we
Prepared using weauth.cls

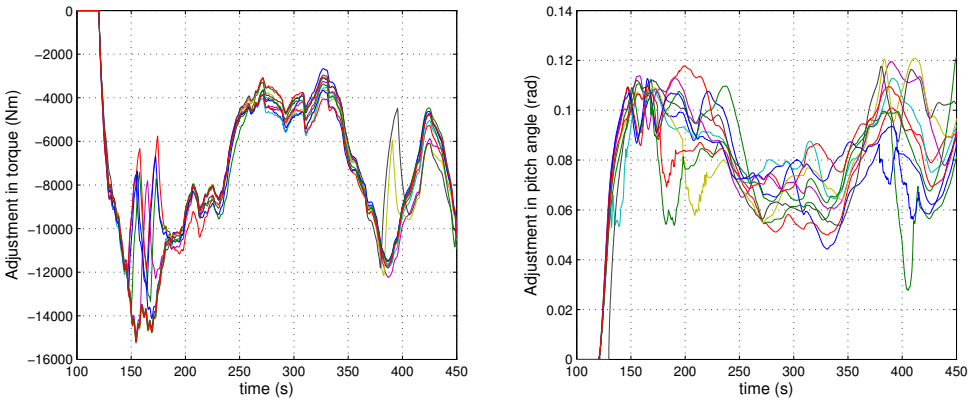

Figure 24. Adjustments in torque (left) and pitch (right).

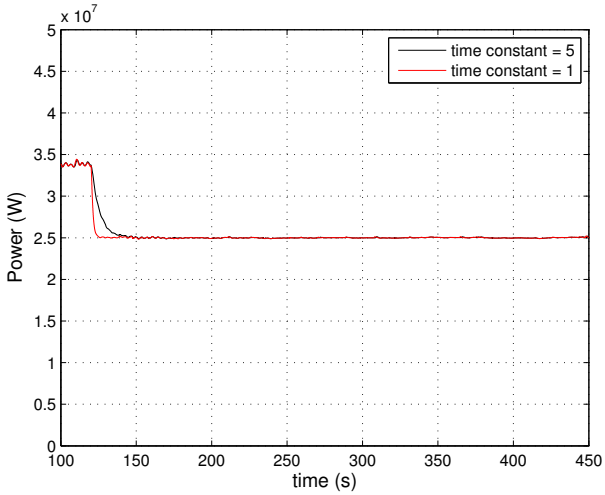

Figure 25. Power adjustment at different speeds.

4.4. Communication Delay

The communication delay between the TWFC and the wind farm has been assumed to be zero throughout the paper. However, this may not always be feasible in real life. The impact of different communication delays, i.e. 0 s, 4 s (2 s each way), 8 s (4 s each way) and 12 s (6 s each way), on the wind farm power output is depicted in Figure 26. $V_r(t)$ is still within 10 % for the largest communication delay of 12 s. It would be even smaller for a wind farm with a larger number of turbines as depicted earlier in Figure 22 and eventually be negligible for wind farms with many tens of turbines; that is, large fluctuations in the wind farm power output would be avoided by ensuring that the number of turbines in the wind farm is sufficiently large and that the communication delay is reasonably small (although the restriction on the communication delay can be relaxed as the wind farm size increases).

The performance of each turbine can be observed from Figure 27, which depicts T_e on the torque/speed plane for different communication delays. As communication delay increases, the reaction time to the changes in flags increases, causing the turbines to operate outside the green zone more frequently. Nonetheless, the turbines still operate within the amber zone even for the largest communication delay of 12 s. Note that the results would be enhanced for a wind farm with a larger number of turbines.

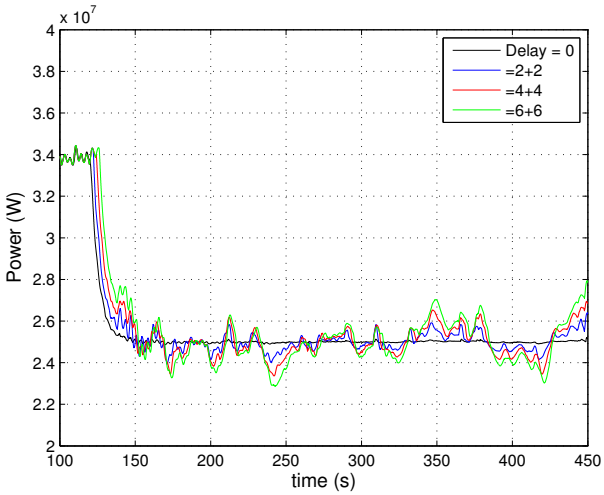

Figure 26. Adjusted power for different communication delays.

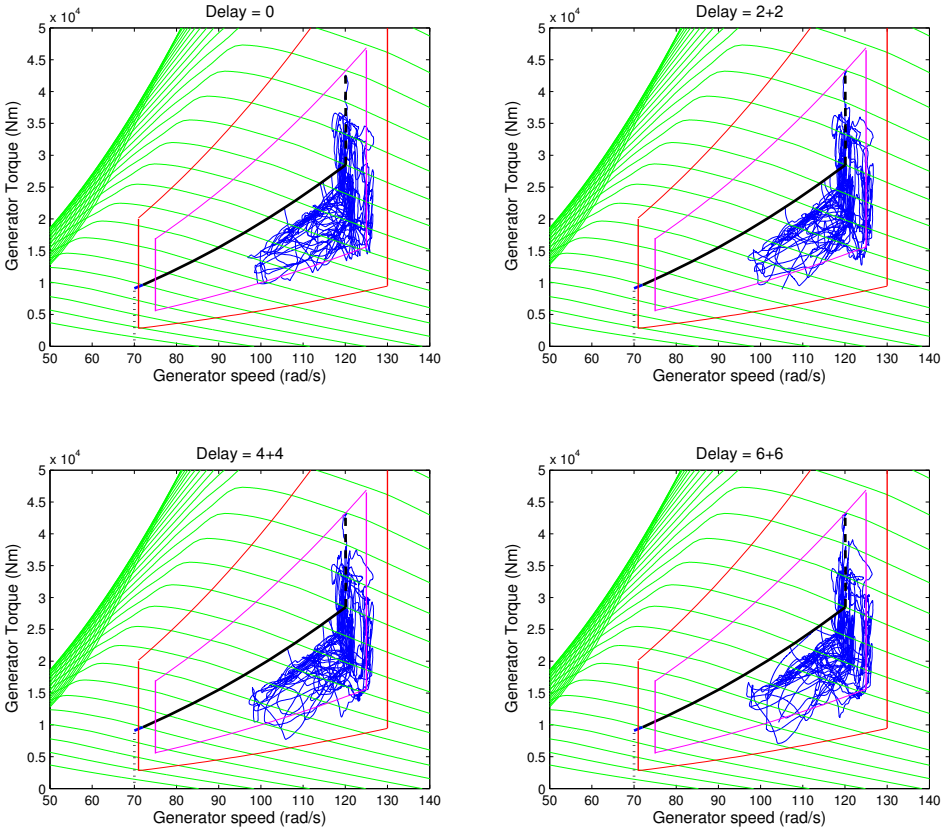

Figure 27. Behaviour of the turbines for different communication delays.

Power spectra of fore-aft TBM, side-to-side BBM and fore-aft BBM are depicted for different communication delays in Figures 28, 29 and 30, respectively. As the spectra are almost identical in each figure, it could be concluded that communication delay has little impact on the operation of the full envelope controllers of each turbine.

Wind Energ. 2014; **00**:1–22 © 2014 John Wiley & Sons, Ltd.
DOI: 10.1002/we
Prepared using weauth.cls

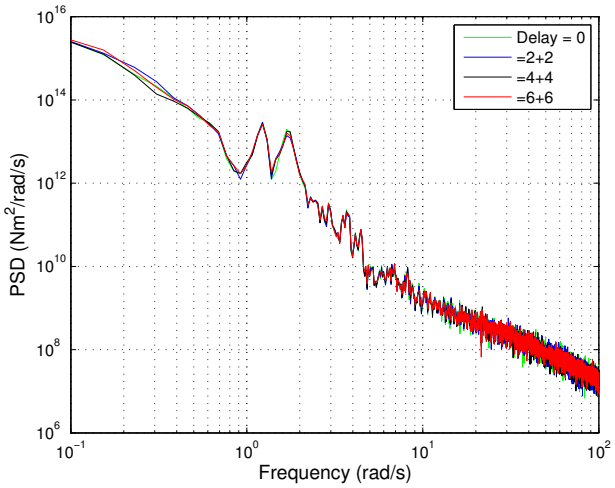

Figure 28. Spectra of fore-aft tower bending moment for different communication delays.

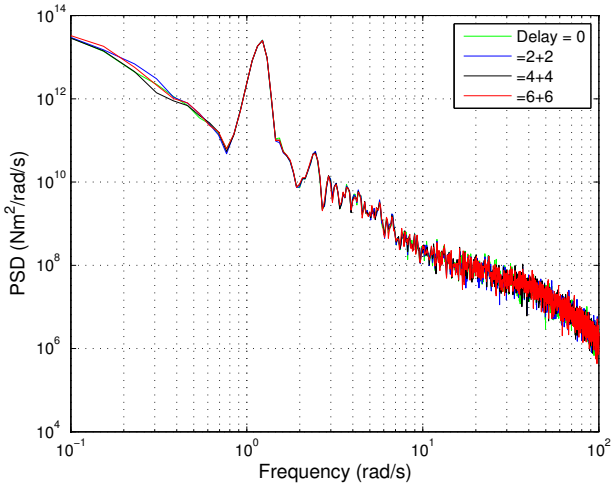

Figure 29. Spectra of fore-aft blade bending moment for different communication delays.

5. CONCLUSIONS

A flexible, hierarchic, decentralised and scalable wind farm controller, capable of providing fast and accurate control of the wind farm power output to meet the wind farm power demand as determined by the grid side operation requirements for the wind farm, is introduced. It utilises an existing full envelope controller and the PAC that has been developed to provide fully flexible operation of an individual turbine. The wind farm controller, by the use of the PAC, causes the power generated by each turbine to be adjusted to regulate the wind farm power output to match the grid requirements, taking into account the status and the operating state of each turbine. The operating state of each turbine is assumed to be equal in this paper.

The simulation results in Matlab/SIMULINK® and BLADED demonstrate that the wind farm power output could be curtailed for an unlimited period of time to match the wind farm power demand while keeping each turbine in a safe operating region by the use of thresholds defined on the torque/speed plane. The allocation and reallocation of the

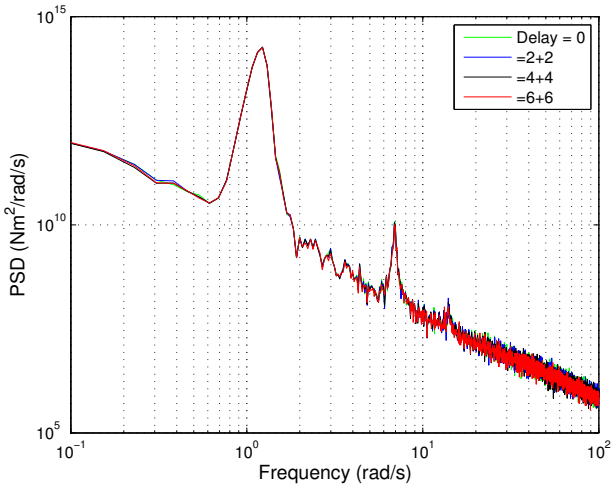

Figure 30. Spectra of side-to-side blade bending moment for different communication delays.

power adjustments between the turbines takes place in a smooth manner, which avoids the introduction of large transients, discontinuities and steps in the wind farm power output. Hence, the resulting power output is smooth.

By curtailing the wind farm power output as opposed to curtailing individual turbine power outputs independently from each other, improved results are attained by allowing those turbines seeing higher wind speeds to compensate for those turbines seeing lower wind speeds. The wind farm controller is also utilised for providing additional power output for a limited period of time. When providing an additional power output, the control algorithm of the wind farm controller is modified for improved results; that is, the turbines cascading towards the red zone is prevented by imroving the algorithm in Section 3.3.

The wind farm controller is also analysed in the frequency domain utilising power spectra to demonstrate that the wind farm controller does not cause a significant feedback effect that could compromise the effectiveness of the turbines full envelope controllers. A simple mathematical proof is also presented. With a larger number of turbines in the wind farm, the feedback effect becomes even weaker. The simulation results also demonstrate that the impact of the communication delay on the operation of the full envelope controller is small. The communication delay needs to be substantially large to cause considerable fluctuations (i.e. $V_r(t)$ from equation (11)) in the wind farm power output, especially for a wind farm with a larger number of turbines. It is also illustrated that the speed of the wind farm controller could readily be altered, which would be essential when providing the turbines with a synthetic inertia response, for instance.

ACKNOWLEDGEMENT

The authors wish to acknowledge the support of the EPSRC for the Supergen Wind Energy Technologies Consortium, grant number EP/H018662/1. The authors are grateful to Adam Stock for providing the PAC and a contribution to Appendix A and the Supergen Wind Energy Technologies Consortium for providing the models of the Supergen 5 MW exemplar turbine.

A. POWER ADJUSTING CONTROLLER RULES

The PAC supervisory rules are implemented in the PAC to ensure that the turbine is kept in a safe operating regime. The occurrence of events triggered by these rules is communicated between the PAC and wind farm controller using flags. (Capital letters are used to indicate flag names with sub-flags in brackets.) There are two sets of rules, black rules defined by a boundary on the torque/speed plane that act as a hard limit and traffic light rules, defined by two concentric boundaries contained within the black rules boundary, that act as soft limits. The boundaries apply to both aerodynamic torque and drive-train torque. The regions inside the inner boundary, between the inner and outer boundaries and outside the outer boundaries are designated green, amber and red, respectively.

General supervisory rules:

- To turn off the PAC, the OFF flag is set by either the PAC or the wind farm controller and the PAC goes into recovery mode. The speed of the recovery can be fast or slow as chosen by the wind farm controller through setting the RECOVERY (Fast/Slow) flag. The default is RECOVERY (Fast). During the recovery mode, the REJECTION (Recovery) flag is set by the PAC.
- Only black supervisory rules apply to high priority events, such as requests for synthetic inertia. The PRIORITY flag is set by the wind farm controller.
- During high turbulence intensity, the PAC is turned off and the REJECTION (Turbulence) flag set by the PAC.
- If actuator pitch rate limits are violated by the turbine full envelope controller, the PAC is turned off and the REJECTION (Actuator) flag set by the PAC with no time limit applied.
- If the turbine state is unstable such that normal operation is unreachable, the UNSTABLE flag is set by the PAC.

Black supervisory rules:

- The boundary and fixed upper limits to the demanded change in power are set with agreement and cannot be changed without agreement of OEM.
- The boundary cannot be crossed under any circumstances.
- On the turbine state reaching the boundary, REJECTION (Limit) flag is set.
- If the turbine state remains on the boundary beyond the pre-set time limit then the PAC is turned off and the PAC goes into RECOVERY mode.
- On a section of the boundary corresponding to the maximum possible generator reaction torque, the permitted time limit before turning off the PAC is zero.

Traffic light supervisory rules:

- The boundaries can be set by wind farm controller.
- The maximum change of power for the red region is zero. Subject to the fixed upper limit, the maximum change of power for the green and amber regions can be set by the wind farm controller with the latter less than the former.
- When the turbine state is in the green/amber/red region, the GREEN/AMBER/RED flag is set by the PAC.
- When the demanded change in power exceeds the maximum, the GREEN (Limit)/AMBER (Limit)/RED (Limit) flag is set by the PAC.

REFERENCES

1. The European Wind Energy Association. Wind in power: 2013 European statistics. *Technical Report*, The European Wind Energy Association 2014.
2. Systems E, Eltra. Wind Turbines Connected to Grids with Voltages above 100 kV: Technical regulation for the properties and the regulation of wind turbines. *Technical Report*, Elkraft Systems and Eltra 2004.

3. Kristoffersen JR. The Horns Rev Wind farm and the Operational. Experience with the Wind Farm Main Controller. *Copenhagen Offshore Wind 2005, 26-28 October*, 2005.
4. Knudsen T, Bak T, Svenstrup M. Survey of wind farm control–power and fatigue optimization. *Wind Energ.* 2014; :1–19.
5. Schepers JG, van der PSP. Improved modelling of wake aerodynamics and assessment of new farm control strategies. *Journal of Physics: Conference Series 75* 2008; .
6. Jeong Y, Johnson K, Fleming P. Comparison and testing of power reserve control strategies for grid-connected wind turbines. *Wind Energ.* 2014; .
7. Chatzopoulos A. Full Envelope Wind Turbine Controller Design for Power Regulation and Tower Load Reduction. PhD Thesis, University of Strathclyde 2011.
8. Stock A. Flexibility of operation. *Supergen wind energy technologies consortium report*, Department of Electronics and Electrical Engineering, University of Strathclyde 2013.
9. Stock A. Providing grid frequency support using variable speed wind turbines with augmented control. *Proceedings of the European Wind Energy Association (EWEA) Conference, Copenhagen, Denmark*, 2012.
10. Gonzalez-Longatt F, Chikuni E, Stemmet W, Folly K. Effects of the synthetic inertia from wind power on the total system inertia after a frequency disturbance. *2012 IEEE Power Engineering Society Conference and Exposition in Africa (PowerAfrica)* 2012; :1–7.
11. Burton T, Sharpe D, Jenkins N, Bossanyi E. *Wind Energy Handbook*. John Wiley & Sons, Ltd, 2001.
12. Bianchi FD, Battista HD, Mantz RJ. *Wind Turbine Control Systems: Principles, Modelling and Gain Scheduling Design*. Springer, 2006.
13. Leithead W, Connor B. Control of variable speed wind turbines: Design task. *International Journal of Control* 2000; **73: 13**:1189 – 1212.
14. Leithead W, Connor B. Control of variable speed wind turbines: Dynamic models. *International Journal of Control* 2000; **73: 13**:1173 – 1188.
15. Leithead WE. Effective wind speed models for simple wind turbine simulations. *Proceedings of* 14^{th} *British Wind Energy Association (BWEA) Conference, Nottingham*, 1992.
16. Munteanu I, Bratcu AI, Cutululis NA, Ceangă E. *Optimal Control of Wind Energy Systems: Towards a Global Approach*. Springer, 2007.

DOI: 10.1002/we
Prepared using weauth.cls